

Langmuir Study of Octadecyltrimethoxysilane Behavior at the Air–Water Interface

S. Vidon and R. M. Leblanc*

Department of Chemistry, University of Miami, 1301 Memorial Drive, P.O. Box 249118,
Coral Gables, Florida 33124

Received: October 14, 1997

The behavior of octadecyltrimethoxysilane ($C_{18}TMS$) at the air–water interface for different subphases pH has been studied through surface pressure–area and surface potential–area isotherms combined with Brewster angle microscopy. $C_{18}TMS$ monomolecular behavior has been assigned to the one observed at pH around 8.0. Hydrolysis or hydrolysis followed by condensation occurs when pH is lowered below 5.0. Hydrolysis followed by condensation is also observed when the pH is raised above 10.5. The type of catalysis predominantly influences the product of the reaction. Condensation is performed at low pH under two constraints: steric hindrance between the C_{18} tail chains and electrostatic repulsion between polar groups, resulting in a very low or nil polymerization degree of the condensation products around the isoelectric point (pH 3.8). Higher concentration of chloride ions gradually inhibits the second constraint, resulting in the formation of a linear polymer. Only steric hindrance has been observed under basic catalysis, producing a monodimensional polymer similar to the one obtained at low pH.

Introduction

The high asymmetry of interfaces is expected to lead to the growth of a polymer when compared to the one taking place in isotropic medium. One-dimensional and two-dimensional polymers could be obtained at interfaces with monomers forming higher dimension products when the reaction is carried out in a three-dimensional phase.^{1,2} Moreover, the presence of two phases enables a more versatile control of the reaction.² Thus, new polymer structures and polymer materials can be prepared, and evaluation of the different parameters controlling the reaction is achievable for a better understanding of the reaction mechanism.

Polymerization of different monomers has been recently studied at interfaces to obtain two-dimensional polymer materials,^{1,3–6} called two-dimensional gels in order to extend the sol–gel process terminology to that new class of materials. Such association is not hazardous since the two kinds of materials tend to have the same applications.^{7–9} Indeed, high optical transparency and tailored-sizes porosity are the properties expected. The alkoxysilanes category is one of the most common class of precursors used in the preparation of three-dimensional gels. Hydrolysis and condensation of precursors result in a three-dimensional polysiloxane network, whose expansion can be controlled to obtain either colloidal particles or bulk gels.¹⁰ Thus, a similar network of lower dimensionality is expected at the air–water interface with amphiphilic alkoxysilanes precursors such as $C_{18}TMS$.

Amphiphilic molecules spread at the air–water interface can be, in a first approximation, considered thermodynamically as a two-dimensional system. Then, the innermost features of the system can be inferred from Langmuir isotherms, using the set of the universal laws of thermodynamics.

Octadecyltrimethoxysilane behavior at the air–water interface has been studied in isothermal conditions (293 K), in compres-

sion, in the 1.4–12.8 pH range. Transverse dielectric properties of the system have been quantified using surface potential measurements, and optically homogeneous domains present on the water surface have been visualized with a Brewster angle microscope.

Experimental Materials and Methods

Octadecyltrimethoxysilane (90% purity) has been supplied by Fluka Chemical (Ronkokoma, NY) and was used without any further purification. *n*-Hexane (99.9%) used as spreading solvent and glycerol (>99.5%) were furnished by Aldrich (Millwaukee, WI). $C_{18}TMS$ source and its solutions were stored under argon, and FTIR measurements were periodically carried out to control their purity, which turned out to be stable in those conditions over long period of time (15 days).

All the glassware was cleaned with detergent FL 70 (Fisher, Pittsburgh, PA), dipped in sulfochromic acid for 30 min, then washed with aqueous sodium hydroxide (0.1 M), and dried in an oven (100 °C) beforehand.

Water has been deionized (resistivity = 18 M Ω .cm, surface tension = 72.6 mN/m, pH = 5.7 at 20 \pm 1 °C) with a Modulab 2020 water purification system (Continental Water Systems Corporation, San Antonio, TX). The pH was adjusted with aqueous solutions of hydrochloric acid or sodium hydroxide and measured with a glass electrode pH meter (Accumet model 10, Fisher, Pittsburgh, PA).

Langmuir isotherms were obtained on a KSV minitrough (450 \times 150 \times 4 mm³, KSV 5000, KSV Instruments, Helsinki, Finland). The surface pressure was measured with a Wilhelmy balance. Surface potential experiments were carried out on a homemade trough (1000 \times 120 \times 6 mm³, compression assured by two symmetrically movable barriers), outfitted with an americium (²⁴¹Am) ionization electrode as a probe and a platinum electrode as reference. A Brewster angle microscope (EMM633S, Nippon Laser & Electronics Lab., Nagoya, Japan, 10 mW helium–neon laser) was mounted on a Nippon Trough

* Corresponding author. E-mail: mmodrono@umiami.ir.miami.edu.

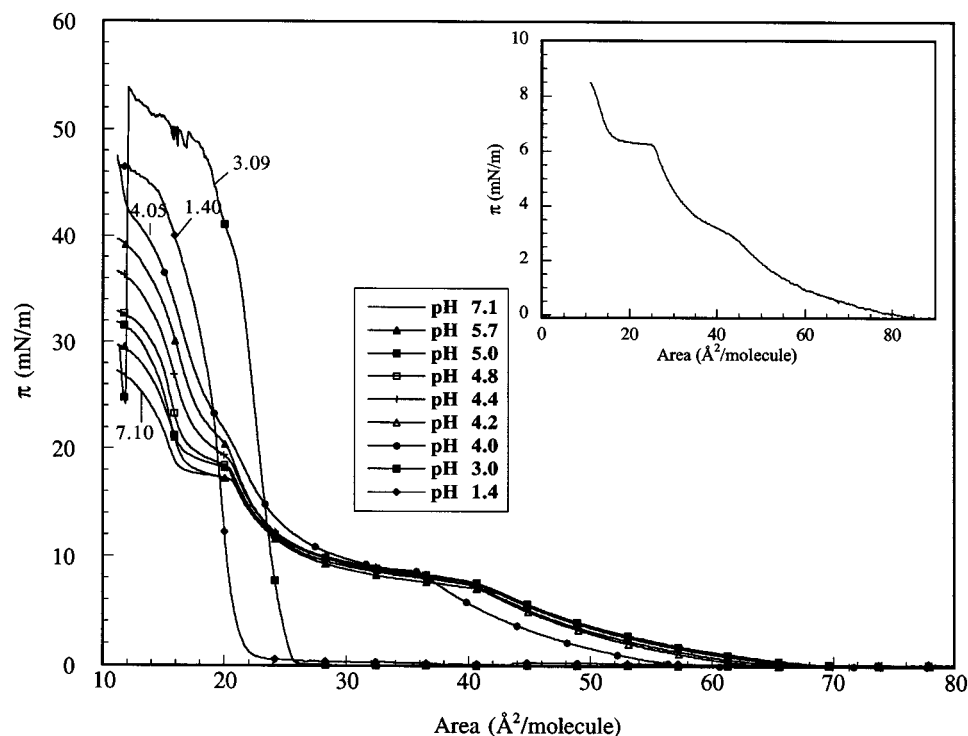


Figure 1. Langmuir isotherms of $C_{18}TMS$ spread on water at different acidic pH. Insert: Langmuir isotherm of $C_{18}TMS$ on glycerol.

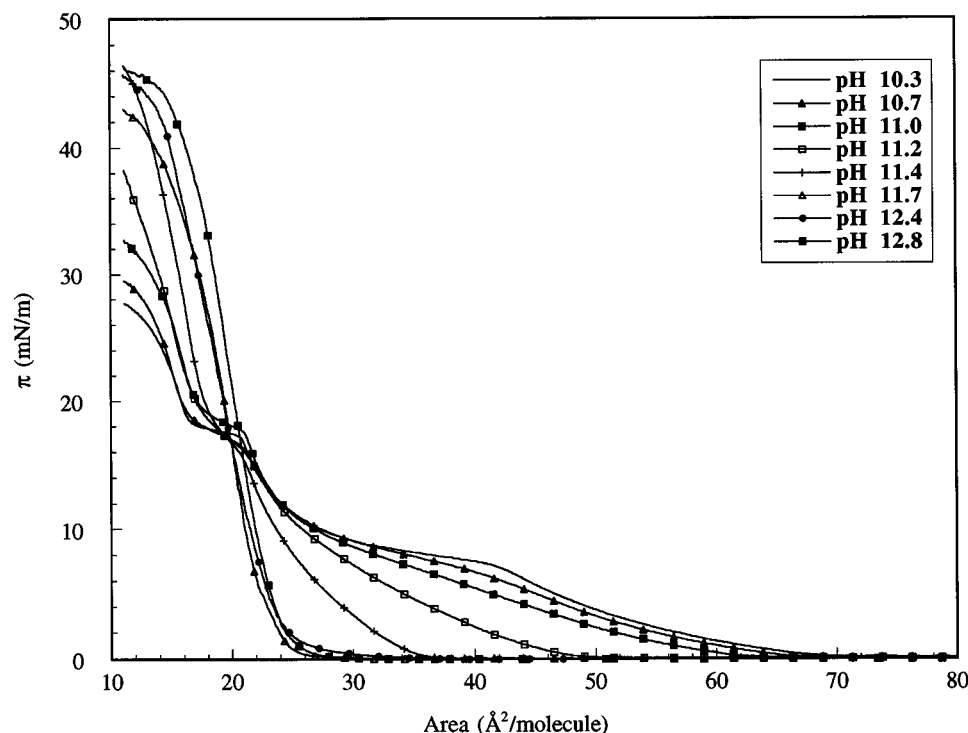


Figure 2. Langmuir isotherms of $C_{18}TMS$ spread on water at different basic pH.

equipped with a moving wall ($440 \times 50 \times 4 \text{ mm}^3$, NL-LB140S-MWC, Nippon Laser & Electronics Lab., Nagoya, Japan). Images were recorded with a CCD camera, digitized with a video capture peripheral (Snappy Video Snapshot, Rancho Cordova, CA), and treated with a low pass band filter (NIH Image 1.62) to remove noise.

All the experiments were carried out in a Class 1000 clean room (temperature $20 \pm 1^\circ\text{C}$, relative humidity $50 \pm 1\%$).

Langmuir isotherms obtained on the different troughs were identical when the same experimental conditions were used, i.e.,

initial molecular area $100 \text{ Å}^2 \text{ molecule}^{-1}$, barrier speed $2.5 \text{ Å}^2 (\text{molecule min})^{-1}$, waiting time after spreading 10 min.

Experimental Results

Langmuir Isotherms. Langmuir isotherms of $C_{18}TMS$ at the air–water interface at different pH of the subphase are shown in Figures 1 and 2. The isotherms have been separated in two sets for convenience and to point out the obvious differences in the behavior of $C_{18}TMS$ when compressed on acidic or basic subphases.

All the isotherms obtained in the pH range 4.8–10.3 exhibit the same features. A liquid expanded (LE) phase is noted in the 42–70 Å² molecule⁻¹ range, followed by a first plateau located at around 9 mN/m and which spans the 27–42 Å² molecule⁻¹ molecular area range. A less compressible phase is noted in the 23–27 Å² molecule⁻¹ range, identified as being a liquid condensed phase (LC), and is the least compressible phase observable on the isotherm. A transition is noted in the interval 18–23 Å² molecule⁻¹, whose shape is much more influenced by change in pH than the one of the first plateau. Isotherms obtained on pure water at different temperatures (not shown here) demonstrate clearly that the first plateau is a first-order phase transition, even though the second is a collapse, usually noticed on fatty acid esters isotherms. It has been shown that such a collapse is due to a steric repulsion of the bulky polar headgroups.¹¹

The first-order phase transition can be interpreted in the following way. Interactions between the C₁₈TMS molecules at the air–water interface at pH 8.0 are only of the van der Waals type. C₁₈ fatty acid molecules at the air–water interface form domains due to their aggregation caused by van der Waals interactions.¹¹ Such domain formation requires a constructive interaction between the headgroup and the water surface, because the molecules are almost perpendicular to the interface in that state. When the head is less hydrophilic like C₁₈TMS, a minimal work, furnished by compression, is mandatory to overcome their instability in such domains, hence the first-order phase transition. On the other hand, when the hydrophobicity of the headgroup is exalted by lengthening the alkoxy chains, the domains become gradually totally unstable at 293 K. Then, for a certain critical alkoxy chain length the first-order phase transition must disappear. Moreover, a shortening of the tail chain must result in an increase of the surface pressure at which the phase transition is observed and a decrease of the length of the plateau, characterizing a gas–liquid-phase transition of the van der Waals type. Thus, the formation of the LC phase is due to constructive interactions between tail chains, but liquid properties are kept since the headgroups do not tend to form a condensed phase, but a gaseous one, contrary to what has been proposed elsewhere.⁵ This assumption becomes obvious when we compare the compressibility modulus of the different LC phase formed at pH between 3.0 and 4.8. It will be shown that hydrolysis occurs in that pH range, and the headgroup is gradually stabilized. Then, the properties of the phase tend to the one of a condensed phase due to van der Waals interactions between the tails.

The Langmuir isotherm of C₁₈TMS on glycerol has been established in order to determine its pure monomolecular behavior (see insert in Figure 1). Indeed, all the isotherms on water present the same features in the 4.8–10.3 pH range, but some differences exist, especially at low molecular area obviously due to the change of the subphase pH. Glycerol has been used for its hydrophilicity and its relatively high surface tension (63.4 mN/m at 20 ± 1 °C). Even though glycerol is hygroscopic, water absorbed forms complexes with glycerol, resulting in a large decrease of its dissociation constant (20 wt % H₂O absorption in glycerol in our clean room, dielectric constant equal to 52.27).¹² Oxonium and hydroxide concentrations, i.e., the major parameters influencing the shape of the isotherms, are expected to be low. The C₁₈TMS Langmuir isotherm on glycerol presents the same characteristics as those described earlier. However, the collapse plateau is particularly long. Its slope is also near zero. Those two characteristics have been chosen to determine the subphase pH at which C₁₈TMS behaves

like its pure monomolecular form. This pH has been found to be around 8.0, and the isotherm obtained at this pH has been chosen as reference to which the others will be compared. When the pH is decreased from 8.0 to 4.8, we note a progressive increase not only of the LC phase compressibility modulus but also of the respective location of the isotherms: the pressure difference between the isotherms and the reference gradually increases from the highest molecular area to the lowest. Nevertheless, the length of the collapse plateau does not change, but its slope increases.

Striking changes are observable for subphase pH below 4.8, and the general behavior is the one of a system presenting a phase separation between C₁₈TMS monomolecular form and a condensed phase. Indeed, the isotherms can be considered as a superposition of two isotherms:¹¹ the one related to the pure monomolecular form and a condensed phase of low compressibility. At pH 3.0, the C₁₈TMS isotherm presents a condensed phase of low compressibility, collapsing at 39 mN/m. The corresponding molecular area is high (25 Å² molecule⁻¹). Moreover, the film obtained at this pH is rigid since the surface pressure decreases drastically under further compression at 12 Å² molecule⁻¹. Such behavior is not observable with films prepared at lower subphase pH. The isotherms are also different. The molecular area at which the collapse is observed decreases down to 20 Å² molecule⁻¹, and an inflection point is noticeable at around 20 mN/m, which characterizes a viscoelastic film.¹³ Polymers are also certainly formed at this pH.

When the pH is increased from 8.0 to 12.8 (Figure 2), the evolution of the isotherms is quite different. The isotherms obtained at subphase pH in the range 8.0–10.5 are exactly the same. For pH greater than 10.5, the phase transition gradually disappears. At pH 10.7, a singularity is noticeable at 35 Å² molecule⁻¹, where the isotherm presents an almost zero first derivative and an inflection point, pointing out the presence of a critical point. The phenomenon associated with this is of course an increase of the characteristic length of the correlation function of the density fluctuations. Further increase of the pH reveals a total disappearance of the phase transition. Only the LE phase subsists. Since no phase separation is observable, the transformation undergone by C₁₈TMS does not end up in the formation of a condensed phase, but rather in a outspread oligomer which can only be linear. For pH greater than 11.7 the isotherm shows a viscoelastic behavior, quantitatively similar to the one observed at low pH. Results obtained from surface potential and Brewster angle microscopy measurements will help us to interpret the observations described above.

Surface Potential Isotherms. Surface potential isotherms have been established over the whole pH range specified above. The one obtained at pH 7.1 is represented in Figure 3a. Surface potential isotherms of C₁₈TMS established as a function of the pH of the subphase have already been described elsewhere.³ For pH belonging to the 4.8–10.3 range, a first sharp increase is noticeable from 0 to 200 mV, corresponding to a first coherence of the density of the system all over the surface. The surface potential then increased steadily up to 340 mV, reached at 40 Å² molecule⁻¹, which corresponds to the end of the phase transition. Then a change in its slope is noticeable, its evolution becoming sharper, to finally reach ~600 mV at the end of the collapse plateau. At the pH at which condensed phases, viscoelastic or not, are observed, the first increase of the surface potential occurs approximately 5 Å² molecule⁻¹ higher than the molecular area at which the first increase in surface pressure is observable. A plateau is reached at the inflection point molecular area. The maximum designated by the arrow in

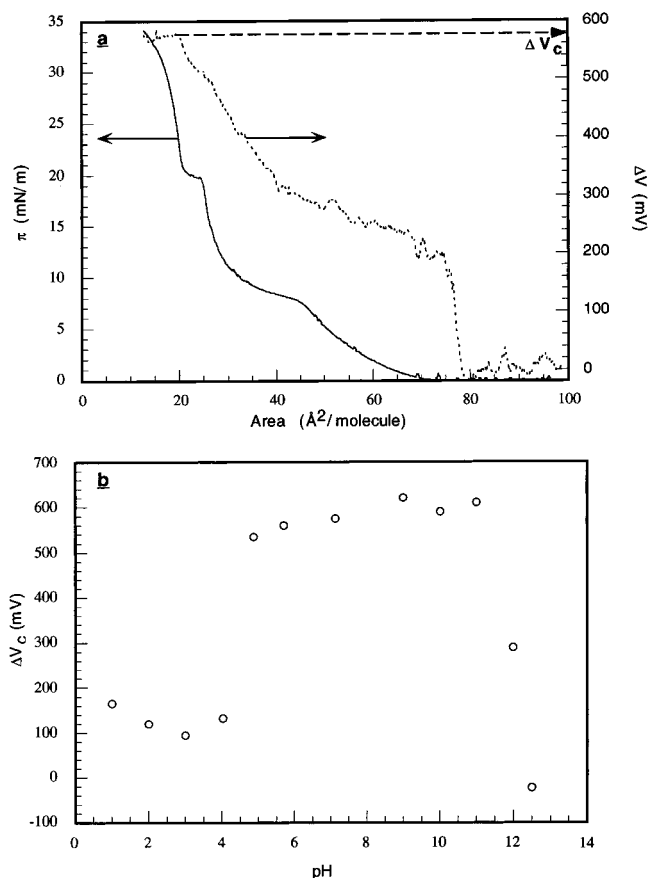


Figure 3. (a) Surface potential isotherm and corresponding Langmuir isotherm of C₁₈TMS on a pH 7.1 subphase. (b) ΔV_c (defined in text) as a function of pH.

Figure 3a has been chosen as parameter to compare the different isotherms and is noted ΔV_c . Also, for pH in the 4.0–12.0 range, ΔV_c corresponds to the molecular area of the end of the collapse plateau. For the others, ΔV_c corresponds to the inflection point molecular area. ΔV_c as a function of pH is shown in Figure 3b. Around the reference pH specified above, ΔV_c slowly decreases from 600 mV before falling down at pH 5.0 and pH 11.0. The isoelectric points is reached at pH 3.8.^{3,10} At pH greater than 12.2, ΔV_c becomes negative, the film being negatively charged. When the pH is decreased from 3.8 to 1.0, ΔV_c steadily increases to reach 200 mV at pH 1.0.

Brewster Angle Microscopy. Brewster angle microscopy (BAM) has been used to visualize optically homogeneous domains formed at the air–water interface. Since the resolution of the microscope is about 1 μm , we did not expect to observe the same features as those observed by Lindén et al.,³ who used epifluorescence microscopy. We rather focus on the influence of pH on the domain shape formed during the first-order phase transition. All the BAM images have been taken during compression, at subphase pH equal to 9.2 (Figure 4, a.1 and a.2), 10.7 (Figure 4.b.1), and 4.2 (Figure 4.c.1). Since pH 9.2 is within the range mentioned above, pictures taken at this pH will act as references.

Image a.2 of Figure 4 has been recorded before the phase transition. No specific feature is observable. It has been inserted to show the effective modifications occurring during the phase transition. Such changes are noticeable on image a.1. Droplike domains are arranged in an ordered manner. Their shape is roughly circular, which shows the liquid character of the phase formed during the transition. Their diameter,

estimated from the corresponding plot profile, is approximately equal to 24 μm .

Image b.1 of Figure 4 has been taken during compression on a pH 10.7 subphase at the molecular area indicated by the arrow on the corresponding isotherm. The same domains as those noticed at pH 9.2 are observable, but the diameter deduced from the profile plot reveals a net increase from the reference one, its value reaching 32 μm . Thus, the liquefaction is induced over longer length scale. This fact corroborates the observation reported earlier, namely, the characteristic length of the correlation function of the density fluctuations is enhanced at this pH.

Image c.1 (Figure 4) has been taken at the end of the transition plateau. Two regions are distinguishable. The first one located at the top of the image is a large homogeneous domain, contrary to the region located at the bottom of the picture, which is formed of small circular domains, similar in shape and in dimensions to those observed at pH 9.2. This observation confirms the phase separation reported above, deduced from the Langmuir isotherms. Also, the two coexisting phases are monomolecular C₁₈TMS and a condensed phase whose nature will be discussed in the following section.

Discussion

We showed in the previous section that a quantification of changes of C₁₈TMS behavior at the air–water interface requires to set the pH as being the determining parameter. Nevertheless, we must keep in mind that chloride or sodium ions were added in the subphase, and their concentrations must also be considered as other parameters.

Kinetic experiments, carried out at constant molecular area (50 Å² molecule⁻¹, initial surface pressure 8.5 mN/m), have been reported elsewhere³ and reproduced in our lab. A nucleation growth process has been observed with a decrease in surface pressure which depends on the pH of the subphase. At pH around the reference one, small changes in surface pressure, about 0.4 mN/m, are observed after an exposure of 1 h. Moreover, the results point out that the phenomenon is exalted at pH 4.0 and 11.0, at which the surface pressure vanishes within 50 min. The relaxation time falls down to 5 min at pH below 4.0 and above 11.5. Furthermore, when the compression is carried out 16 h after spreading on a pure water subphase (pH 5.7), the isotherm obtained is the one of a condensed phase.

An analytical evaluation with ESCA of the chemical composition of C₁₈TMS films deposited on glass using the Langmuir–Blodgett¹⁵ technique at pH 1.0, 5.7, and 11.0 has been described elsewhere.⁴ The results show that the condensed phases observed at pH 1.0 and 11.0 are exempt of methoxy groups. Such characteristics have also been observed at pH 5.7 after a longer exposure of the film to the subphase. C₁₈TMS is then either hydrolyzed or polymerized in the condensed phases (viscoelastic or not).

Thus, since the compression lasts 35 min, the isotherms obtained at intermediate pH (4.8–10.5) characterize unhydrolyzed C₁₈TMS, whereas the isotherms obtained in the narrow pH ranges 3.9–4.8 and 10.3–11.7 correspond to partially hydrolyzed species or partially hydrolyzed and condensed species. Those obtained at pH below 3.9 and above 11.7 characterize totally hydrolyzed species or totally polymerized species.

The isotherms obtained at pH subphases in the 10.3–11.7 range are characterized by a gradual disappearance of the phase transition. A critical point has been noticed at pH 10.7, from

which we inferred the presence of a linear oligomer. The surface potential in that pH range is still positive, indicating that the film is still uncharged. This is in accordance with the fact that hydrolyzed C₁₈TMS is a weak acid, due to the positive inductive effect of the tail hydrocarbon chain.¹⁰ Negative charges carried by the film are noticeable from pH 12.2. Therefore, the condensation product is formed under one constraint only: the steric hindrance of the hydrocarbon chains, as has been shown elsewhere from geometrical considerations.⁴ At pH greater than 12.2, at which the film is negatively charged, the Langmuir isotherms are those of a condensed phase and are similar to those observed in the 11.7–12.2 pH range. Thus, the charge of the film seems to have no influence on the geometry of the product, as screened by sodium counterions.

We pointed out that isotherms established at pH in the 4.8–8.0 range only differ in their relative position, especially when the system is in the LC phase. We also reported that hydrolysis is effective in the 1.0–4.8 pH range, since the Langmuir isotherms as well as the surface potential isotherms present a drastic change in that region. It is also known that the second plateau corresponds to a collapse of the film which occurs at the head level. We also remarked that the length of the plateau decreases from pH 4.8 to completely disappear at pH 3.0. Thus, the length of the plateau can be used to measure the hydrolysis rate of the film.

We noticed that the length of the plateau is constant over the whole 4.8–10.3 pH range, but its slope increases from pH 8.0 to pH 4.8. We also observed that the difference in surface pressure between the isotherms obtained at pH 8.0 and pH 4.8 gradually increases from the highest molecular area to the molecular area at which the collapse occurs. Such an effect is ascribed to electrostatic repulsion. Since the absolute potential of the film is negative, because of the basicity of the oxygens of the methoxy groups, adsorption of oxonium ions occurs, and their density at the interface grows when their concentration is increased in the subphase. Such adsorption is observable on the surface potential isotherm and especially in Figure 3.b, where ΔV_c slowly decreases when oxonium concentration is increased. The charge effect is maximum at pH 4.8.

The inverse of the difference in surface pressure between the isotherms obtained at pH 4.8 and at pH 8.0, $1/\Delta\Pi$, as a function of the molecular area is shown in Figure 5.a. This function decreases to reach a minimum at the molecular area at which collapse occurs. The extrapolation to zero gives a molecular area equal to 20 Å² molecule⁻¹, which is assumed to be the fictive area at which the charges are in contact. Since the oxygens are the basic sites and are in a sp³ hybridization state, the locations of oxonium ions that correspond to those three criteria are shown in Figure 5.b. Three oxonium ions are adsorbed on each headgroup when the system is in the LC phase. The locations are perfectly symmetric and correspond to a saturation of all the basic acceptor sites available, and this is true all over the surface.

It is striking that such saturation is observable at pH slightly higher than those at which the hydrolysis rate is enhanced. This fact can be interpreted in the following way. The TMS head is slightly hydrophobic and does not interact constructively with water. Hence, the angle between the plane formed by the three oxygens of the methoxy groups and the interface is not zero. A further increase in the oxonium concentration of the subphase increases the potential of the its surface, resulting in a decrease of the angle mentioned above. The equilibrium value of the angle mentioned above results from a balance between two major contributions: the distribution of charges in the subphase

corresponding to an equilibrium state of the subphase, taking into account the boundary conditions imposed by the presence of the layer; the energy of the electric field generated by the charges present in the vicinity of the interface.

The last contribution is minimal when the charge at the interface is zero and is possible if and only if it is compatible with a plausible boundary condition of the charge distribution in the subphase. However, it occurs at the isoelectric point of the monolayer. Hence, the stabilization of the headgroup at the interface by the oxonium ions is effective for pH lower or equal to the isoelectric point of the C₁₈TMS.

The stabilization process enhanced the hydrolysis rate because it facilitates the approach of a water molecule to the silicon atom. Hence, oxonium ions catalyze the hydrolysis reaction in stabilizing the headgroup at the interface and bringing silicon and water into contact.

At pH 4.8, the oxonium concentration is still too low to permit a stabilization in the LE phase, for which a further increase of the potential of the surface of the subphase is mandatory. But adsorption is observable in the LC phase, since the angle mentioned above is lowered during the LC phase formation, due to compression. Also, since the only observable phenomenon enhanced by the increase of oxonium concentration is their adsorption at the surface of the film, the drastic evolution of the behavior must be due to such antagonism.

Moreover, since the angle mentioned above vanishes during the LC phase formation, as well as during the stabilization of the headgroup due to the increase of the subphase surface potential, the head configuration in the LC phase at pH slightly higher than the stabilizing one is similar to the one in the LE or gaseous phases at pH lower than the stabilizing one. We can consider the first state as a mimic, at the head level, of the second state, since the heads are constrained to adopt an identical configuration just before their collapse by compression. Thus, the location of the oxonium adsorption sites should be the same in those two states.

Electrostatic repulsion of the head and steric hindrance of the hydrocarbon chains are two constraints which must influence the condensation reaction in acidic catalysis. We already mentioned that the isotherms and BAM images of C₁₈TMS spread on subphase pH belonging to the 4.0–4.8 range show a phase separation between unhydrolyzed C₁₈TMS and a solid phase. Such a condensed phase, if formed by condensation of C₁₈TMS, has lattice parameters that are determined by the constraints imposed during its growth. It is also formed via condensation of C₁₈TMS if the hydrocarbon tails and the charges lattices are compatible. Since the latest one must be hexagonal, Figure 6 shows that such compatibility is impossible. Then, the condensed phase observed should be formed by hydrolyzed C₁₈TMS. Indeed, from the basic catalyzed condensation examination, we know that the only steric hindrance generates a linear polymer that is soluble in the unhydrolyzed C₁₈TMS phase, and such a phase separation would not be observable. Moreover, the hydrolyzed species behaves like a fatty acid at the interface and forms a condensed domain, hence the phase separation. The necessary weakness of the condensation rate around the isoelectric point can be understood in another manner. Since the condensation reaction requires the collision of two C₁₈TMS molecules, the positive charge carried by the head should decrease the collision rate and thus lower the condensation rate.

A further increase of hydrochloric acid concentration increases the chloride ions density at the interface. This adsorption enables us to interpret the increase of ΔV_c in Figure 3.b from

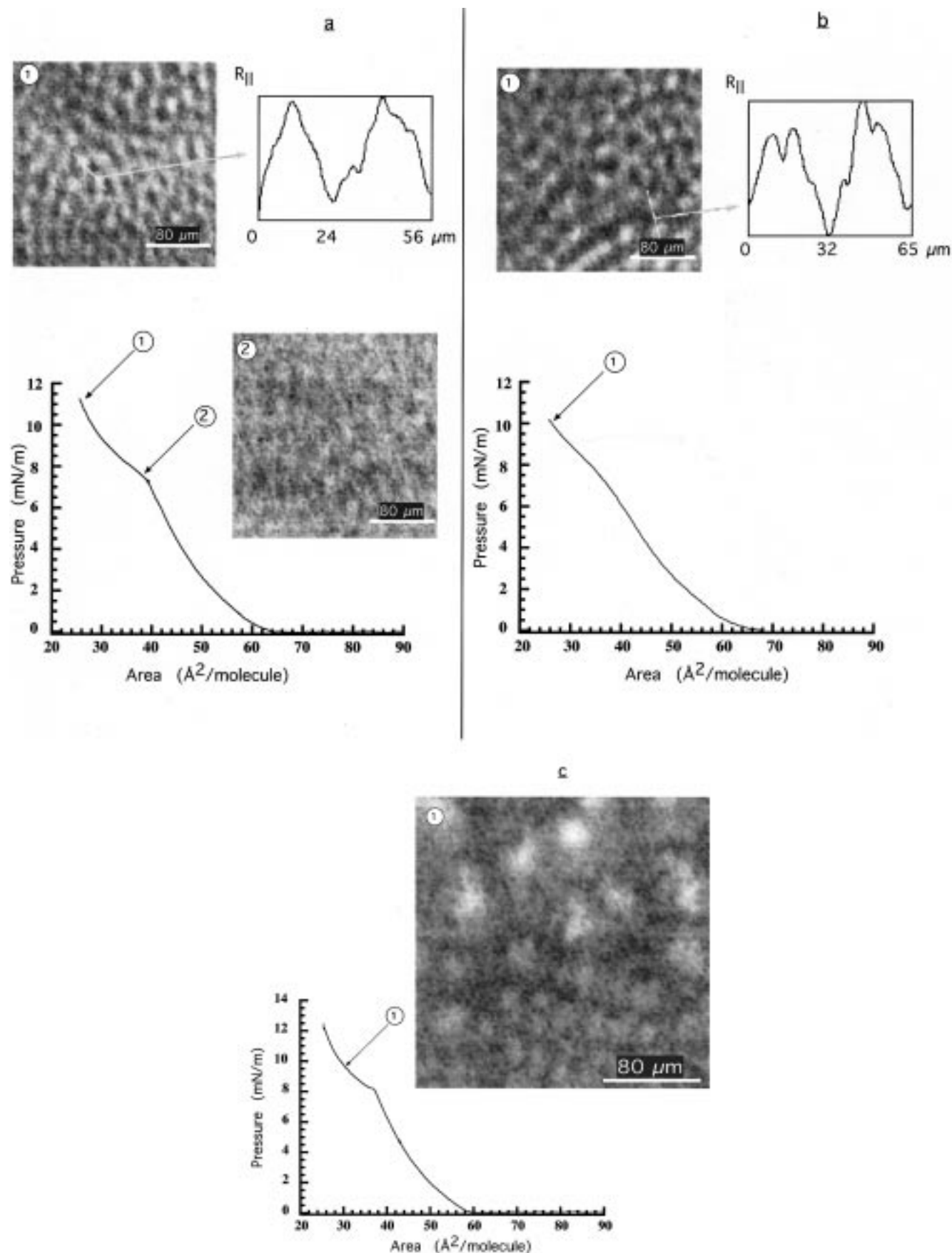


Figure 4. Brewster angle microscopy images of $C_{18}TMS$ on water taken at the molecular areas designated by the arrows. The pH of the subphase was adjusted at 9.2 (a), 10.7 (b), and 4.2 (c). The profile plot has been drawn (reflectivity of the parallel electric field component as a function of the position on the segment drawn in the corresponding image) for images taken during compression on pH 9.2 and 10.7 subphases.

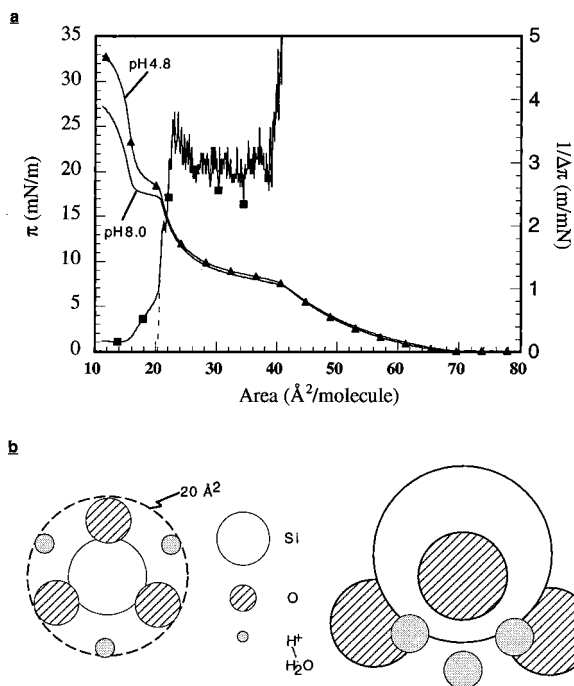


Figure 5. Evaluation of the charge effect observed at pH 4.8. (a) The inverse of $\Delta\pi$, defined as the difference between the isotherms obtained at pH 4.8 and pH 8.0 (reference), is represented as a function of the molecular area. The extrapolation at zero surface pressure before film collapse is assumed to be the fictive molecular area at which the charges are in contact. (b) Corresponding geometrical model.

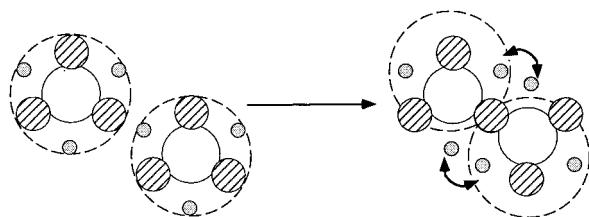


Figure 6. Molecular representation showing that condensation of two C₁₈TMS molecules cannot fulfill the two following criteria, deduced from the observation of a phase separation, i.e., the formation of a solid phase: tail chains steric hindrance and hexagonal lattice necessary formed by the charges.

pH = 3.8 to 1.0. Such adsorption weakens the electrostatic repulsion between C₁₈TMS molecules, increasing the collision rate. Thus, for low pH, the electrostatic constraint has not been taken into account, and the condensation reaction is only influenced by hydrocarbon tails steric hindrance as in the basic catalyzed case. Indeed, the same viscoelastic behavior as the one observed at high pH has been noticed at low pH. Hence, the reaction products should be the same at those pHs.

The screening effect of the adsorbed chloride ions is corroborated by the Langmuir isotherm obtained at pH 3.0, on which the presence of the hydrolyzed C₁₈TMS species and the polymerized one is noticeable. The Langmuir isotherm shows a sharp increase of the surface pressure up to 40 mN/m followed by a slight inflection before increasing and falling sharply. The inflection observed at 40 mN/m occurs at the same surface pressure as the viscoelastic film collapse. Moreover, the way the second collapse occurs is similar to those of fatty acids. Then the film formed at pH 3.0 should contain the C₁₈TMS condensed form and the hydrolyzed form, the first one forming the most compressible phase.

The weakness of the condensation rate at pH around the isoelectric point finds an analogy in the three-dimensional case.

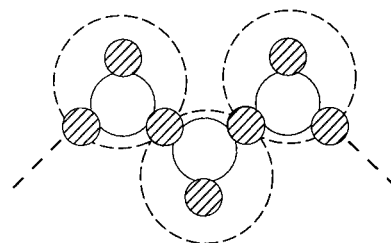


Figure 7. Structure of the linear polymer formed through hydrolysis and condensation of C₁₈TMS.

It has been reported elsewhere that the gelation time of poly-(silicic acid) sols reaches a maximum in the acidic pH range.¹⁰ Such an observation has two interpretations. The first one has been proposed by Iler¹⁰ and was based on the possibility of a condensation reaction catalyzed by fluoride ions at low pH. This fact has been denied by Klimentova and Kirichenko,¹⁴ who proved that this maximum occurs at the isoelectric point of the particles and suggested that such an effect should be associated with a strong adsorption of water molecules on the particles surface. Our analysis enables us to formulate another interpretation for this phenomenon. Since the condensation rate of the hydrolyzed species is minimum when the adsorption sites described above are all engaged by oxonium ions, and when the counterions concentration is low enough to avoid a screening of their repulsive effect, the stabilization of poly(silicic acid) sols could be due to the formation of an oxonium Stern layer at their surfaces, built up in the same manner as the one observed at the air–water interface.

Conclusion

A linear polymer is obtained through a hydrolysis–condensation reaction when C₁₈TMS is spread on a basic subphase. On acidic subphases, C₁₈TMS reacts with water to form the hydrolyzed species or the condensed one, depending on the concentration of the acidic compound in the subphase and its ionic strength. The condensed species formed in those conditions are also linear and have the same structure as the one formed in basic conditions. The linearity of the polymer is due to the steric hindrance of the hydrocarbon tail chains. Moreover, the behavior of such a polymer is viscoelastic. Thus, the chains adopt a random coil conformation. Since the hydrocarbon chains orient the product geometry, they should be divided on both sides of the chains in an ordered manner, as shown in Figure 7. They are also in a random coil conformation. But it is well-known that the trans configuration is more probable at lower temperature. Such an effect should be enhanced if the length of the chain is shorter. Since chains interact constructively, the trans conformation of the C₁₈ chains must influence the geometry of the polysiloxane chain by straightening it up. Also, a thermotropic liquid-crystalline phase transition is expected. Since polysiloxane chains are expected to be semiconducting, such properties could find numerous applications.

We should mention that the interpretations formulated above found a corroboration in preliminary results we obtained with other amphiphilic alkoxysilanes. Such results have not been included here and will constitute the topic of a future article.

Acknowledgment. We acknowledge all the members of our research group for their daily assistance. This work was supported by the Research Office of the Department of the Army under Contract 36479-CH.

References and Notes

- (1) Moriguchi, I.; Maeda, H.; Teraoka, Y.; Kagawa, S. *J. Am. Chem. Soc.* **1995**, *117*, 1139.
- (2) Hiemenz, P. C. *Polymer Chemistry*; Decker Inc.: London, 1984.
- (3) Lindén, M.; Slotte, J. P.; Rosenholm, J. B. *Langmuir* **1996**, *12*, 1449.
- (4) Sjöblom, J.; Stakkestad, G.; Ebeltof, H.; Friberg, S. E.; Claesson, P. *Langmuir* **1995**, *11*, 2652.
- (5) Taylor, D. M.; Gupta, S. K.; Dynarowicz, P. *Thin Solid Films* **1996**, *284–285*, 80.
- (6) Ge, S.; Takahara, A.; Kajiyama, T. *Langmuir* **1995**, *11*, 1341.
- (7) Lev, O.; Tsiosky, M.; Rabinovitch, L.; Glezer, V.; Sampath, S.; Pankratov, I.; Gun, J. *Anal. Chem.* **1995**, *67*, 22A.
- (8) Avnir, D.; Braun, S.; Lev, O.; Ottolenghi, M. *Chem. Mater.* **1994**, *6*, 1605.
- (9) *Sol–Gel Technology of Thin Films, Fibers, Preforms, Electronic and Specialty Shapes*; Klein, L. C., Ed.; Noyes Publications: Park Ridge, NJ, 1988.
- (10) Iler, R. K. *The Colloid Chemistry of Silica and Silicates*; Wiley: New York, 1979.
- (11) Gaines, G. L., Jr. *Insoluble Monolayers at Liquid–Gas interfaces*; 1966.
- (12) Newman, A. A. *Glycerol*; CRC Press: Cleveland, OH, 1968.
- (13) Davies, J. T.; Rideal, E. K. *Interfacial Phenomena*; Academic Press: London, 1961.
- (14) Deryagin, B. V. *Research in Surface Forces*; Consultant Bureau: New York, 1975; Vol. 4, p 77.
- (15) Blodgett, B. B. *J. Am. Chem. Soc.* **1935**, *57*, 1007.